ЖЭТФ, 1999, том 115, вып. 2, стр. 449–462

ATOM COOLING BY VSCPT: ACCUMULATION PLUS FILTERING

Fam Le Kien[a,b], *V. I. Balykin*[a,c*]

[a] *Institute for Laser Science, University of Electro-Communications Tokyo 182, Japan*

[b] *Department of Physics, University of Hanoi, Hanoi, Vietnam*

[c] *Institute of Spectroscopy, Russian Academy of Sciences 142092, Troitzk, Moscow Region, Russia*

Submitted 2 December 1997,
Resubmitted 7 September 1998

We study laser cooling by velocity-selective coherent population trapping (VSCPT) in a double-Λ scheme with decay beyond the working levels. We show that this additional decay channel filters diffused atoms from trapped ones and provides an ultrasharp atomic momentum distribution.

1. INTRODUCTION

Coherent population trapping was observed for the first time by Alzetta et al. [1] as a decrease in fluorescent emission in a laser optical pumping experiment involving a three-level atomic system with two ground levels and one excited level. This effect results from coherent superposition of the ground states which is stable against absorption from the radiation field. Various theoretical and experimental aspects of coherent population trapping have been reviewed in several papers [2–6]. This phenomenon has been exploited in very different applications: metrology, optical bistability, high-resolution spectroscopy, laser multiphoton ionization, four-wave mixing, laser-induced structures in the continuum, laser manipulation of atoms, adiabatic transfer, lasing without inversion, and matched pulse propagation.

The application of velocity-selective coherent population trapping (VSCPT) to laser manipulation of atoms has been studied intensively [7–18]. The basic idea of VSCPT is to pump atoms into a noncoupled state that has a well-defined momentum, where the atoms do not interact with the laser radiation. Accumulation of atoms in this special velocity-selective trapping state is due to spontaneous emission. In VSCPT experiments [7–10] with ^{4}He metastable atoms, very narrow final distributions of atomic momenta are observed. The form and width of the momentum distribution has been described theoretically for various schemes and in various regimes [11–18]. It is common to associate either the peak width or the dark-state population of an atomic momentum distribution with an effective temperature. Based on this effective temperature, the authors of Refs. [7–18] conclude that laser cooling below the recoil limit has been achieved. However, spontaneous emission produces, as shown in these references, not only the accumulation of atoms in the trapping state but also diffusion

*E-mail:: balykin@isan.troitsk.ru

of some those atoms toward high values of momentum. Unlike the velocity-selective trapping phenomenon, the diffusion of atoms in the momentum space tends to increase the temperature. Due to such a random process, the wings of the momentum distribution are not Gaussian. In the meantime, the wing shape and the fraction of the atoms that have diffused toward the wings are not reflected in the peak width and dark-state population. Consequently, the increase in the peak value and decrease in the width of the final atomic momentum distribution, which is far from Gaussian, do not mean the cooling; they merely indicate the accumulation of atoms in the dark state. A simple analytical description of trapping versus diffusion was recently given in Ref. [19]. A nice way to confine atomic velocities during the VSCPT phase has been proposed by Marte et al. [20]. This method is based on the coexistence of VSCPT and polarization-gradient cooling.

The purpose of this paper is to show that one can use VSCPT to perform not only accumulation but also filtering of atoms in momentum space. Based on the theoretical Λ model of Ref. [11], we introduce a double-Λ model, where an additional upper level with possible decay outside the working configuration is added. We find that this new decay channel can separate the atoms in the wings from atoms near the peaks of the momentum distribution, and hence laser cooling of atoms below the recoil limit can be achieved.

The paper is organized as follows. In Sec. 2 we formulate the model and present the basic equations for the atomic density-matrix elements. In Sec. 3 we perform a numerical analysis. Finally, Sec. 4 contains conclusions.

2. MODEL AND BASIC EQUATIONS

We consider an ensemble of atoms of mass M moving in the z direction. The atoms have two degenerate ground levels, g_- and g_+, and two nondegenerate excited levels, e and e'. We denote the energy of the atomic level j ($j = e, e', g_-, g_+$) by $\hbar\omega_j$. The ground sublevels, g_- and g_+, can be coupled to the level e by two counterpropagating laser beams with the same frequency ω_L, the opposite wave vectors k and $-k$ being aligned along the z direction, and the strengths being characterized by the Rabi frequencies Ω_+ and Ω_-, see Fig. 1. Similarly, the level e' can also be coupled to the levels g_- and g_+ by two counterpropagating laser beams with frequency ω'_L and strengths characterized by the Rabi frequencies Ω'_+ and Ω'_-. The second pair of laser beams is aligned in the z' direction, which may be different from the z direction, but should be very close. We denote the projections of the wave vectors of these laser beams onto the z axis by k' and $-k'$. In what follows we are interested only in the atomic center-of-mass motion along the z axis. We take into account the spontaneous emission of atoms from the upper levels e and e' to the ground sublevels g_- and g_+. In addition, we assume that the level e' can decay into another level, which is not shown in the figure. Furthermore, the fields can

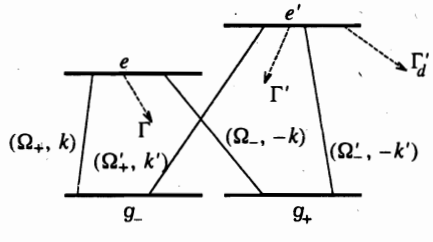

Fig. 1. Energy levels and optical transitions in the double-Λ configuration

be switched on and off at different times, that is, the Rabi frequencies Ω_+, Ω_-, Ω'_+, and Ω'_- are generally functions of time.

We introduce the state $|j,p\rangle$, which represents an atom in the internal state j with linear momentum p along the z axis. Because of momentum conservation, the interaction of the atom with the fields can couple $|e,p\rangle$ only with $|g_-,p-\hbar k\rangle$ and $|g_+,p+\hbar k\rangle$, and $|e',p\rangle$ only with $|g_-,p-\hbar k'\rangle$ and $|g_+,p+\hbar k'\rangle$. The Hamiltonian corresponding to the unitary evolution of the system is of the form

$$H = H_A + H_{int}, \tag{1}$$

where

$$H_A = \frac{P^2}{2M} + \hbar\omega_e|e\rangle\langle e| + \hbar\omega_{e'}|e'\rangle\langle e'| \tag{2}$$

describes the translational and internal degrees of freedom of the atom and

$$H_{int} = \sum_p \left(\hbar\Omega_+|e,p\rangle\langle g_-,p-\hbar k| + \hbar\Omega_-|e,p\rangle\langle g_+,p+\hbar k|\right)e^{-i\omega_L t} + \\ + \sum_p \left(\hbar\Omega'_+|e',p\rangle\langle g_-,p-\hbar k'| + \hbar\Omega'_-|e',p\rangle\langle g_+,p+\hbar k'|\right)e^{-i\omega' L t} + \text{H.c.} \tag{3}$$

describes the interaction of the atom with the laser fields, which are taken to be classical.

We assume that an atom in the upper level e can decay into the lower levels g_- and g_+, emitting a fluorescence photon in any direction. This spontaneous emission leads to the damping of the population of e and the associated coherences and to the feeding of g_- and g_+. We assume that the atomic decay rate Γ and the normalized probability $H(u)$ of emitting a photon with momentum u along the z axis do not depend on the center-of-mass motion and are the same for transitions from e to g_- and g_+. Analogously, we assume that an atom in the upper level e' can decay into each of the lower levels g_- and g_+ with the rate Γ'. The corresponding probability of emitting a photon with momentum u along the z axis is denoted by $H'(u)$. In addition, we assume that an atom in the upper level e' can decay with the rate Γ'_d into a fifth level, which is not shown in the figure. This dissipative irreversible decay will remove the untrapped diffused atoms from the working configuration.

Such a filtering process enables us to separate heated atoms from cooled ones, that is, to get a cooled system. The cooling efficiency is determined by the accumulation efficiency from one side and the separation efficiency from the other side. Since the atomic separation efficiency is proportional to the rate Γ'_d of the decay into the outside of the working configuration, we expect that for a subsequent application of the pairs of the laser beams, a higher decay rate Γ'_d will enable us to obtain a cooler atomic system.

We derive in Appendix the generalized optical Bloch equations

$$\frac{d}{dt}\rho_{ee}(p_1,p_2) = \left[\frac{d}{dt}\rho_{ee}(p_1,p_2)\right]_{Ham} + \left[\frac{d}{dt}\rho_{ee}(p_1,p_2)\right]_{\Gamma},$$

$$\frac{d}{dt}\rho_{e'e'}(p_1,p_2) = \left[\frac{d}{dt}\rho_{e'e'}(p_1,p_2)\right]_{Ham} + \left[\frac{d}{dt}\rho_{e'e'}(p_1,p_2)\right]_{\Gamma'} + \left[\frac{d}{dt}\rho_{e'e'}(p_1,p_2)\right]_{\Gamma'_d},$$

$$
\begin{aligned}
\frac{d}{dt}\rho_{\pm\pm}(p_1,p_2) &= \left[\frac{d}{dt}\rho_{\pm\pm}(p_1,p_2)\right]_{Ham} + \left[\frac{d}{dt}\rho_{\pm\pm}(p_1,p_2)\right]_{\Gamma} + \left[\frac{d}{dt}\rho_{\pm\pm}(p_1,p_2)\right]_{\Gamma'}, \\
\frac{d}{dt}\rho_{e\pm}(p_1,p_2) &= \left[\frac{d}{dt}\rho_{e\pm}(p_1,p_2)\right]_{Ham} + \left[\frac{d}{dt}\rho_{e\pm}(p_1,p_2)\right]_{\Gamma}, \\
\frac{d}{dt}\rho_{e'\pm}(p_1,p_2) &= \left[\frac{d}{dt}\rho_{e'\pm}(p_1,p_2)\right]_{Ham} + \left[\frac{d}{dt}\rho_{e'\pm}(p_1,p_2)\right]_{\Gamma'} + \left[\frac{d}{dt}\rho_{e'\pm}(p_1,p_2)\right]_{\Gamma'_d}, \\
\frac{d}{dt}\rho_{-+}(p_1,p_2) &= \left[\frac{d}{dt}\rho_{-+}(p_1,p_2)\right]_{Ham}, \\
\frac{d}{dt}\rho_{ee'}(p_1,p_2) &= \left[\frac{d}{dt}\rho_{ee'}(p_1,p_2)\right]_{Ham} + \left[\frac{d}{dt}\rho_{ee'}(p_1,p_2)\right]_{\Gamma} + \\
&+ \left[\frac{d}{dt}\rho_{ee'}(p_1,p_2)\right]_{\Gamma'} + \left[\frac{d}{dt}\rho_{ee'}(p_1,p_2)\right]_{\Gamma'_d}.
\end{aligned}
\tag{4}
$$

These equations govern the evolution of the density-matrix elements of the atom with the internal and external degrees of freedom, and will be solved numerically in the next section. Using this numerical solution, we will calculate and study the atomic momentum distribution. We will then calculate the mean deviation of the atomic momentum from the nearest peak, which characterizes the effective temperature of the atomic subsystem.

Note that the above model is very simple, but it can reveal the underlying physics of actual situations, in which atomic level configurations are usually much more complicated. A specific example that is nearest to our model is neon in the metastable $1s_5$ level, with $1s_5$-$2p_9$ and $1s_5$-$2p_2$ transitions and decay channel from $2p_2$ to $1s_3$. This atomic level configuration is used in the laser cooling experiment reported by Shimizu et al. [21]. A scheme to achieve velocity-selective coherent population trapping in a multilevel system under two-frequency laser excitation is proposed in Ref. [18]. One difference between our model and the model of Ref. [18] is that a trapping state in our model is a superposition of two ground levels, and is created by two laser beams of the same frequency, while a trapping state in the other model is a time-dependent superposition of three ground levels and is created by two-color fields. Moreover, dissipative irreversible decay out of the working configuration plays a significant role in our model, while the authors of Ref. [18] considered only decay from the excited levels to the ground levels.

3. NUMERICAL ANALYSIS

We now study numerically the generalized optical Bloch equations (4) for the case in which the laser detunings $\delta_L = \omega_L - \omega_e$ and $\delta'_L = \omega'_L - \omega_{e'}$ are zero and the spontaneous-emission rates from the upper levels to the ground sublevels are equal ($\Gamma = \Gamma'$). We choose, for our example, an atomic mass M and the wave number k such that the recoil frequency $\omega_{rec} \equiv \hbar k^2/2M$ is $\omega_{rec} = 0.027\,\Gamma$, which corresponds to the experiment [7] on He atoms. The decay rate Γ'_d of the atoms from the level e' into the outside of the double-Λ configuration is chosen to be $\Gamma'_d = .10\Gamma$. Since the atomic separation efficiency is proportional to Γ'_d, the value chosen for this parameter is good enough to demonstrate filtering, and consequently, cooling the atoms below sub-recoil energy for reasonable interaction times. For a significantly higher or lower value of Γ'_d, the cooling efficiency, which depends on the rate of separation of heated and cooled atoms, is, in the case of subsequent application of the pairs laser beams, expected to

be higher or lower, respectively. The temporal evolution is obtained by incrementation starting from various initial conditions. The time increment is $0.01\Gamma^{-1}$, small enough to avoid artificial instabilities introduced by the incremental approach. Since the exact shapes of the kernels $H(u)$ and $H'(u)$, characterizing the spontaneous-radiation patterns, are not important [11], we take the constant forms $H(u) = 1/2\hbar k$ and $H'(u) = 1/2\hbar k'$.

For the initial atomic state, we take a statistical mixture of the two ground sublevels, g_- and g_+, with momentum distribution

$$W_0(p) = \frac{1}{\sigma\sqrt{2\pi}} \exp\left(-\frac{p^2}{2\sigma^2}\right), \tag{5}$$

which is a normalized Gaussian function with a peak at $p = 0$ and a standard width σ. The initial density-matrix elements $\rho_{j_1 j_2}(p_1, p_2)\Big|_{t=0}$ are thus vanish, except for

$$\begin{aligned} \rho_{--}(p,p)\Big|_{t=0} &= \frac{1}{2} W_0(p), \\ \rho_{++}(p,p)\Big|_{t=0} &= \frac{1}{2} W_0(p). \end{aligned} \tag{6}$$

For the standard width of the initial momentum distribution we choose the value $\sigma = 3\hbar k$. The variable p is discretized in steps of $\epsilon = \hbar k/30$, from $-p_{max}$ to p_{max}, where $p_{max} = 30\hbar k$. The chosen value of ϵ is small enough compared to the narrowest structure that emerges in the solution of Eqs. (4). The chosen value of p_{max} is large enough that the interesting part of the solution (near $p = 0$) for the largest value of t considered here ($t = 600\,\Gamma^{-1}$) is not affected by the truncation of the p range. For such values of p_{max} and t, the momentum diffusion from p values larger than p_{max} to $p = 0$ is negligible.

We are interested in the momentum distribution of those atoms that have not decayed from the double-Λ configuration at the end of the interaction with the laser fields. The probability density of finding such an atom with linear momentum p along the z axis is

$$W(p) = \rho_{ee}(p,p) + \rho_{e'e'}(p,p) + \rho_{--}(p,p) + \rho_{++}(p,p). \tag{7}$$

Due to the decay of the atoms from the double-Λ configuration, the function $W(p)$ is not normalized with respect to the variable p. When we integrate this function over p, we obtain the probability

$$W_{remain} = \int_{-\infty}^{\infty} W(p)dp, \tag{8}$$

that an atom remains in one of the working levels. The normalized function

$$W_{norm}(p) = \frac{1}{W_{remain}} W(p) \tag{9}$$

is the momentum distribution corresponding to the sub-ensemble of atoms that remain in the working levels after the interaction with the fields.

In order to characterize the effective temperature in the cooling process, we introduce the quantity

$$V \equiv \left\{ \int_{-\infty}^{\infty} [p - p_{max}(p)]^2 W_{norm}(p) dp \right\}^{1/2}, \tag{10}$$

which is the mean deviation of the atomic momentum p from the nearest peak $p_{max}(p)$. The effective temperature of the atomic system is defined as

$$\theta_{eff} \equiv V^2/2M. \tag{11}$$

The sub-recoil cooling occurs when $\theta_{eff} < \theta_{rec}$ where $\theta_{rec} \equiv (\hbar k)^2/2M$ is the recoil energy.

The deviation V characterizes the statistical spread of the atomic ensemble in momentum space. However, the geometrical peak width and the dark-state population used to characterize VSCPT [7, 11] correspond only to a part of the ensemble. This is the principal difference between our effective temperature and the effective temperature used in VSCPT [7, 11].

When the momentum distribution $W_{norm}(p)$ has only one peak p_{max}, which is, due to the symmetry of the initial conditions and the evolution equations, positioned at the mean momentum $\bar{p} = 0$, the quantity V coincides with the momentum standard deviation,

$$V^2 = \int_{-\infty}^{\infty} p^2 W_{norm}(p) dp = \int_{-\infty}^{\infty} (p - \bar{p})^2 W_{norm}(p) dp, \tag{12}$$

and characterizes the spread of the atoms around the peak as well as the spread of the whole momentum distribution.

When the central peak at $p = 0$ splits into two symmetrical side peaks positioned at $\pm p_0$ ($p_0 > 0$), we can consider the system of the atoms that remain in the working level configuration after the interaction with the fields as a two-component system, one component with $p \geq 0$ and the other component with $p \leq 0$. Note that the normalized momentum distributions of these two components are $2W_{norm}(p \geq 0)$ and $2W_{norm}(p \leq 0)$, respectively. Hence, we see from the expression

$$V^2 = 2 \int_{0}^{\infty} (p - p_0)^2 W_{norm}(p) dp \tag{13}$$

that V characterizes the spread of the atoms around each peak, as well as the spread of the momentum distribution of each component.

In what follows, we show and discuss numerical results for the case in which the two pairs of laser beams are applied in succession. The detailed sequence is the following. The first pair of laser beams resonant with the transitions $e \leftrightarrow g_-$ and $e \leftrightarrow g_+$ is turned on for the time T and then shut down. The second pair of laser beams resonant with the transitions $e' \leftrightarrow g_-$ and $e' \leftrightarrow g_+$ is then turned on for the time T'. The time-dependent Rabi frequencies corresponding to the laser pulses in each pair are taken to be the same, and have the rectangular forms

$$\begin{aligned} \Omega_- &= \Omega_+ = \Omega_0[\theta(t) - \theta(t - T)], \\ \Omega'_- &= \Omega'_+ = \Omega'_0[\theta(t - T) - \theta(t - T - T')]. \end{aligned} \tag{14}$$

Here, Ω_0 and Ω'_0 are the maximal values of the Rabi frequencies, and $\theta(t)$ is the Heaviside step function.

We have solved Eqs. (4) for the parameters $\Omega_0 = \Omega_0' = 0.3\Gamma$, $T = 150\Gamma^{-1}$, and $T' = 450\Gamma^{-1}$ for two different cases: $k' = k$ and $k' = 1.1k$. According to Aspect et al. [11], the peak width of the momentum distribution is of order $M\Omega_0/k\sqrt{\Gamma T}$ for the first step, and $M\Omega'_0/k'\sqrt{(\Gamma' + \Gamma_d)T'}$ for the second. We therefore expect that the chosen interaction times $T = 150\Gamma^{-1}$ and $T' = 450\Gamma^{-1}$ are large enough to show two resolved peaks at the end of the first step and two very narrow peaks at the end of the second. For larger values of T and T', the effect becomes more dramatic.

3.1. The case of $k' = k$

We first present results for equal wavenumbers, that is, the case when $k' = k$. We show by the dashed and the solid curves in Fig. 2 the probability density $W(p)$ for an atom to have momentum p at times $t = T$ and $t = T+T'$, respectively, while remaining in the double-Λ level configuration. Since the decay out of the double-Λ configuration occurs only when the second pair of laser beams is turned on, the probability density $W(p)$, which corresponds to the original ensemble, and the normalized momentum distribution $W_{norm}(p)$, which corresponds to the sub-ensemble of atoms inside the working configuration, are identical at $t = T$ but different at $t = T + T'$. Therefore, we additionally plot the function $W_{norm}(p)$ obtained at $t = T + T'$ by the dashed-dotted curve. For comparison, the initial momentum distribution $W_0(p)$ is denoted by a dotted curve.

The dashed curve in Fig. 2 shows that the atomic momentum distribution obtained at the end of the interaction with the first pair of the laser beams exhibits two resolved peaks emerging at $\pm\hbar k$ above the initial distribution [11]. Such a structure results from the accumulation of atoms in the state

$$|\Psi_0\rangle = \frac{1}{\sqrt{2}}\left(|g_-, -\hbar k\rangle - |g_+, \hbar k\rangle\right), \tag{15}$$

which is a velocity-selective coherent trapping state with respect to the first pair of laser beams. The mechanism for accumulating atoms in this trapping state is momentum redistribution resulting from the spontaneous emission from the upper level e to the ground sublevels g_- and g_+. Besides the double narrow-peak structure, one sees that some of the atoms have diffused toward higher momentum values. All the above features of the momentum distribution depicted by the dashed curve in Fig. 2 have been studied in details in Ref. [11].

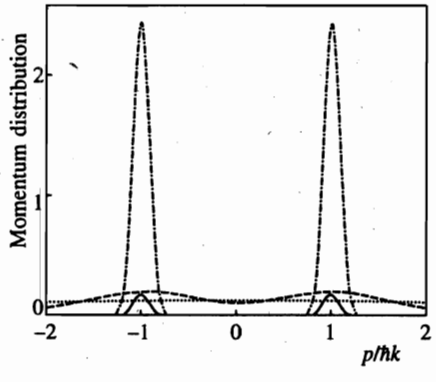

Fig. 2. Atomic momentum distributions produced by the successive application of two pairs of laser beams with equal wavenumbers $k' = k$. The dashed curve illustrates $W(p)$ at the end of the operation of the first pair of laser beams. The solid curve and the dashed-dotted curve correspond to $W(p)$ and $W_{norm}(p)$, respectively, at the end of the operation of the second pair of the laser beams. The dotted curve corresponds to the initial momentum distribution. Here we have chosen the parameters $\sigma = 3\hbar k$, $\Gamma' = \Gamma$, $\Gamma'_d = 10\Gamma$, $\omega_{rec} \equiv \hbar k^2/2M = 0.027\Gamma$, $\Omega'_0 = \Omega_0 = 0.3\Gamma$, $T = 150\Gamma^{-1}$, and $T' = 450\Gamma^{-1}$

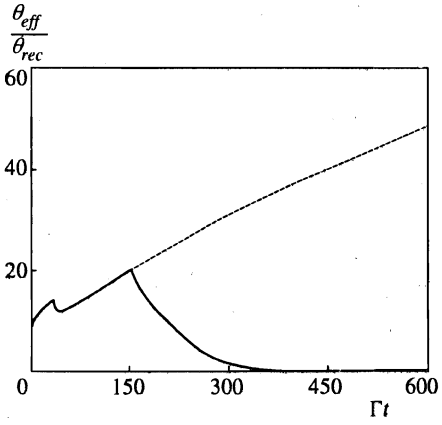

Fig. 3. Temporal evolution of the effective temperature θ_{eff} in units of the recoil energy θ_{rec} for the period of successive application of two pairs of laser beams with equal wavenumbers $k' = k$ (solid curve). All parameters are the same as for Fig. 2. For comparison, the dashed curve represents corresponding values of $\theta_{eff}/\theta_{rec}$ for the case of a single pair of laser beams that operate on an upper level with no decay out of the working configuration

The solid curve in Fig. 2 shows that the second pair of the laser beams take off those atoms whose momenta are not near to $\pm\hbar k$. The spread of the distribution function $W(p)$ with respect to the peaks is greatly reduced, while the peak heights, which have the meaning of the probability densities for an atom from the original ensemble to remain within the working level configuration with linear momentum $\hbar k$ or $-\hbar k$, do not change appreciably. The reason is that when $k = k'$, the state (15) is also a velocity-selective coherent trapping state with respect to the second pair of laser beams, and those atoms which are not in this trapping state at the end of the first stage must undergo decay into the outside of the working level configuration in the second stage. The corresponding probability for an atom to remain in one of the working levels is $W_{remain} \simeq 0.074$.

The dash-dot curve in Fig. 2 shows that the peaks of the normalized momentum distribution $W_{norm}(p)$ created at $t = T + T'$ become not only much narrower but also much higher than the peaks of the dashed curve created at $t = T$. Thus, we observe a decrease in the momentum deviation around the peaks, or in other words cooling of the sub-ensemble of atoms that continue to stay in the double-Λ configuration after the interaction with the two pairs of laser beams. This cooling is due to the accumulation of atoms in the trapping state in combination with filtering of the atoms in momentum space.

In Fig. 3, we plot by the solid line the temporal development of the effective temperature θ_{eff} in units of the recoil energy θ_{rec} for the whole time period of subsequent operation of the two pairs of the laser beams. For comparison, we depict by the dashed line the corresponding values of $\theta_{eff}/\theta_{rec}$ for the case in which the first pair of laser beams continues to operate without the intervention of the second pair for the entire time period [7, 11]. It is worth noting that during the operation of the first pair of laser beams, that is, for the part at $t \leq 150\,\Gamma^{-1}$ for the solid line and for the entire dashed line, the effective temperature θ_{eff} is in general increasing, except for a short time during which a sharp drop, like a phase transition, suddenly occurs. This increase in θ_{eff} is due to atomic momentum diffusion and clearly shows that the atomic system at this stage is not cooled but heated, despite the accumulation of atoms in the dark state. This result is quite different from statements of Refs. [7, 11], where a very similar system was considered but the atomic momentum diffusion was not taken into account in the definition of the effective temperature. The sudden decrease in θ_{eff} occurring for a short time period is associated with the splitting of the central peak into the side peaks, whose locations very quickly move from 0 to $\pm\hbar k$. In other words, this phase-transition-like behavior is a result of the splitting of the atomic system from one component, with the momentum peak at 0, into

two components, with momentum peaks at $\pm\hbar k$. In contrast to the first pair of laser beams, the second pair, operating from $t = 150\,\Gamma^{-1}$ to $t = 600\,\Gamma^{-1}$, causes a monotonic decrease in the effective temperature θ_{eff}. By the end of the interaction, θ_{eff} is approximately $0.0085\,\theta_{rec}$ — a value which is small in comparison with the initial value $9\,\theta_{rec}$ as well as with the recoil energy θ_{rec}. This decrease in the effective temperature is a signature of laser cooling below the one-photon recoil energy. It should be emphasized here that the underlying physics of the cooling obtained here involves velocity-selective coherent population trapping, on the one hand, and the filtering of the atoms in momentum space, on the other.

3.2. The case of $k' \neq k$

We now present numerical results for unequal wavenumbers k' and k. All conditions are the same as in the previous case except that $k' = 1.1\,k$.

In Fig. 4, the solid curve is the probability density $W(p)$ for an atom to have momentum p at time $t = T + T'$, remaining inside the double-Λ configuration of levels. The total probability for an atom to remain inside this configuration is $W_{remain} \simeq 0.035$. The dotted curve represents the initial momentum distribution. The dashed curve represents the probability density $W(p)$ for an atom to have momentum p at time $t = T + T'$ in the case when $k' = k$. As in the case of equal wavenumbers (dashed curve) the probability density function $W(p)$ in the case of unequal wavenumbers (solid curve) is very narrow compared to the initial momentum distribution (dotted curve) and photon momenta $\hbar k$ and $\hbar k'$, and is free from diffusion wings. However, the two peaks resulting from interaction with the second pair of laser beams are now positioned

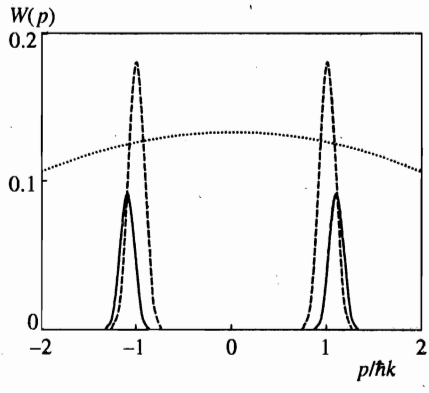

Fig. 4

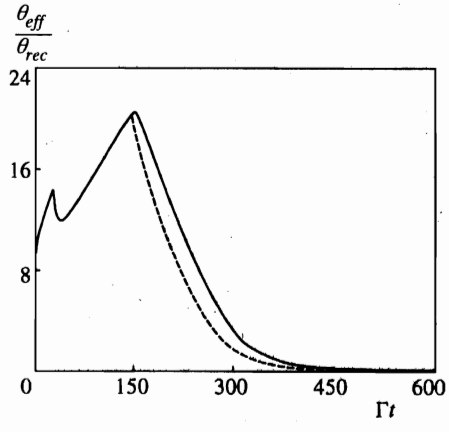

Fig. 5

Fig. 4. Final atomic momentum probability density $W(p)$ in the case of unequal wavenumbers $k' = 1.1\,k \neq k$ (solid curve). All parameters are the same as for Fig. 2. For comparison, we show the initial momentum distribution and the final momentum probability density $W(p)$ in the case of equal wavenumbers $k' = k$ (dotted curve and dashed curve, respectively)

Fig. 5. Temporal evolution of effective temperature θ_{eff} in units of the recoil energy θ_{rec} during successive application of two pairs of laser beams with unequal wavenumbers $k' = 1.1\,k \neq k$ (solid curve). All other parameters are the same as for Fig. 2. For comparison, we show $\theta_{eff}/\theta_{rec}$ for equal wavenumbers (dashed curve)

at $p = \hbar k' = 1.1\hbar k$. Moreover, the peaks of $W(p)$ in the case of unequal wavenumbers (solid curve) are lower than the corresponding peaks in the case of equal wavenumbers (the dashed curve).

The reason is that: when $k' \neq k$, the velocity-selective trapping state

$$|\Psi_0'\rangle = \frac{1}{\sqrt{2}}\left(|g_-, -\hbar k'\rangle - |g_+, \hbar k'\rangle\right) \tag{16}$$

of the atoms interacting with the second pair of laser beams is different from the trapping state $|\Psi_0\rangle$, Eq. (15), of the atoms with respect to the first pair of the laser beams. After interaction with the first pair of laser beams, the number of atoms in the state $|\Psi_0\rangle$, which corresponds to momenta $\pm\hbar k$, is greater than the number of atoms in the state $|\Psi_0'\rangle$, which corresponds to momenta $\pm\hbar k'$. However, the second pair of laser beams takes away the atoms in $|\Psi_0\rangle$ while it does not affect the atoms in $|\Psi_0'\rangle$. This explains the shift in the peak positions from $\pm\hbar k$ to $\pm\hbar k'$, as well as the decrease in the peak heights.

In Fig. 5, we depict by the solid line the time development of the effective temperature θ_{eff} in units of recoil energy θ_{rec} for unequal wavenumbers $k' = 1.1\,k \neq k$. For comparison, we replot (dashed line) the corresponding values of $\theta_{eff}/\theta_{rec}$ for equal wavenumbers $k' = k$. The figure shows that the second pair of laser fields in the case of unequal wavenumbers can also reduce the effective temperature θ_{eff} to a much lower value than the recoil energy θ_{rec}, which is indicative of sub-recoil cooling. During the operation of the second pair, i.e., for $t > 150\,\Gamma^{-1}$, the cooling effect for $k' \neq k$ (solid line) is not as strong as the cooling effect in the case of $k' = k$ (the dashed line). The reason is the difference between the velocity-selective trapping states $|\Psi_0'\rangle$ and $|\Psi_0\rangle$ with $k' \neq k$. This difference leads to the shift in the peaks of the atomic momentum distribution from locations $\pm\hbar k$, created by the first pair of the laser beams, to the locations $\pm\hbar k'$, created by the second pair. Such a process is not favorable for the dark-state population accumulation as well as the cooling of the atoms. Furthermore, we note that the two curves in Fig. 5 tend to merge with each other when $t > 450\,\Gamma^{-1}$. The reason is that after interaction with the second pair of laser beams for a long enough time, the new peak structure of the atomic momentum distribution is well established and most of the atoms having momenta in the diffusion wings are removed. The effective temperature θ_{eff} is then proportional to the peak width, which does not depend on the initial conditions in this limit [11]. This is why the difference in the effective temperature θ_{eff} between the case of $k' \neq k$ and the case of $k' = k$ becomes small when the time of the interaction with the second pair of laser beams is long enough.

4. CONCLUSIONS

We have studied the application of velocity-selective coherent population trapping to laser manipulation of atomic center-of-mass motion in the framework of a simple double-Λ model.

We have introduced a variance of the momentum distribution with respect to the peaks, which can be used to characterize the effective temperature of atoms in the presence atomic momentum diffusion.

We have found that during the operation of the first pair of laser beams, operating in an upper level with no atomic decay out of the working configuration, the effective temperature is in general increasing, except for a short time during which a sharp drop, like a phase transition, suddenly occurs. Such an increase in the effective temperature is due to atomic momentum

diffusion, and indicates heating of the atomic system at this stage in despite of the dark-state population accumulation. The sudden decrease in the effective temperature occurring for a short time is associated with the central peak splitting into two side peaks.

The subsequent application of the second pair of laser beams, operating on the other upper level with possible atomic decay into out of the working configuration, can filter atoms in the wings from the atoms near the peaks of the momentum distribution, cause a monotonic decrease in the effective temperature, and thereby lead to the laser cooling below the one-photon recoil energy.

The difference between the wave numbers of the two pairs of laser beams results in a shift of the peak positions, a decrease in the peak heights, and a decrease in the cooling rate.

Our model is very simple, and has been used just to show the underlying physics of real situations, where atomic level configurations are usually much more complicated. From this model we have seen clearly that (a) the known standard VSCPT scheme does not cool, but, in fact, it heats the whole ensemble of atoms, since the trapped atoms are mixed with the diffused ones, (b) an additional dissipative irreversible decay channel can filter atoms in momentum space, and (c) the use of VSCPT in a combination of accumulation and filtering steps can cool atoms below the recoil energy. To study the cooling effect in a specific real medium, further work will be required.

F. L. K. gratefully acknowledges the support of the Nishina Memorial Foundation and the Vietnamese Basic Research Program in Natural Sciences, and appreciates the hospitality of Prof. K. Shimizu during his stay at the Institute for Laser Science. V. I. B. would like to express his gratitude for the hospitality during his stay at the Institute for Laser Science.

APPENDIX A

Generalized optical Bloch equations

We use the simplified notation

$$\begin{aligned}
\rho_{ee}(p_1,p_2) &= \langle e,p_1|\rho|e,p_2\rangle,\\
\rho_{e'e'}(p_1,p_2) &= \langle e',p_1|\rho|e',p_2\rangle,\\
\rho_{\pm\pm}(p_1,p_2) &= \langle g_\pm,p_1|\rho|g_\pm,p_2\rangle,\\
\rho_{e\pm}(p_1,p_2) &= \langle e,p_1|\rho|g_\pm,p_2\rangle e^{i\omega_L t},\\
\rho_{e'\pm}(p_1,p_2) &= \langle e',p_1|\rho|g_\pm,p_2\rangle e^{i\omega'_L t},\\
\rho_{-+}(p_1,p_2) &= \langle g_-,p_1|\rho|g_+,p_2\rangle,\\
\rho_{ee'}(p_1,p_2) &= \langle e,p_1|\rho|e',p_2\rangle e^{i(\omega_L-\omega'_L)t},\\
\rho_{j_2j_1}(p_2,p_1) &= \rho^*_{j_1j_2}(p_1,p_2),
\end{aligned} \tag{A.1}$$

where $j_1, j_2 = e, e', g_-, g_+$. By using the Schrödinger equation

$$i\hbar\left[\frac{d}{dt}\rho\right]_{Ham} = [H,\rho], \tag{A.2}$$

the equations of unitary evolution for the matrix elements of the density operator ρ are found to be

$$
\begin{aligned}
\left[\frac{d}{dt}\rho_{ee}(p_1,p_2)\right]_{Ham} &= i\frac{p_2^2-p_1^2}{2M\hbar}\rho_{ee}(p_1,p_2)- \\
&- i\Omega_+\rho_{-e}(p_1-\hbar k,p_2)+i\Omega_+^*\rho_{e-}(p_1,p_2-\hbar k)- \\
&- i\Omega_-\rho_{+e}(p_1+\hbar k,p_2)+i\Omega_-^*\rho_{e+}(p_1,p_2+\hbar k), \\
\left[\frac{d}{dt}\rho_{e'e'}(p_1,p_2)\right]_{Ham} &= i\frac{p_2^2-p_1^2}{2M\hbar}\rho_{e'e'}(p_1,p_2)- \\
&- i\Omega'_+\rho_{-e'}(p_1-\hbar k',p_2)+i\Omega'^*_+\rho_{e'-}(p_1,p_2-\hbar k')- \\
&- i\Omega'_-\rho_{+e'}(p_1+\hbar k',p_2)+i\Omega'^*_-\rho_{e'+}(p_1,p_2+\hbar k'), \\
\left[\frac{d}{dt}\rho_{\pm\pm}(p_1,p_2)\right]_{Ham} &= i\frac{p_2^2-p_1^2}{2M\hbar}\rho_{\pm\pm}(p_1,p_2)+ \\
&+ i\Omega_\mp\rho_{\pm e}(p_1,p_2\mp\hbar k)+i\Omega'_\mp\rho_{\pm e'}(p_1,p_2\mp\hbar k')- \\
&- i\Omega^*_\mp\rho_{e\pm}(p_1\mp\hbar k,p_2)-i\Omega'^*_\mp\rho_{e'\pm}(p_1\mp\hbar k',p_2), \\
\left[\frac{d}{dt}\rho_{e\pm}(p_1,p_2)\right]_{Ham} &= i\left(\delta_L+\frac{p_2^2-p_1^2}{2M\hbar}\right)\rho_{e\pm}(p_1,p_2)- \\
&- i\Omega_\mp[\rho_{\pm\pm}(p_1\pm\hbar k,p_2)-\rho_{ee}(p_1,p_2\mp\hbar k)]- \\
&- i\Omega_\pm\rho_{\mp\pm}(p_1\mp\hbar k,p_2)+i\Omega'_\mp\rho_{ee'}(p_1,p_2\mp\hbar k'), \\
\left[\frac{d}{dt}\rho_{e'\pm}(p_1,p_2)\right]_{Ham} &= i\left(\delta'_L+\frac{p_2^2-p_1^2}{2M\hbar}\right)\rho_{e'\pm}(p_1,p_2)- \\
&- i\Omega'_\mp[\rho_{\pm\pm}(p_1\pm\hbar k',p_2)-\rho_{e'e'}(p_1,p_2\mp\hbar k')]- \\
&- i\Omega'_\pm\rho_{\mp\pm}(p_1\mp\hbar k',p_2)+i\Omega_\mp\rho_{e'e}(p_1,p_2\mp\hbar k), \\
\left[\frac{d}{dt}\rho_{-+}(p_1,p_2)\right]_{Ham} &= i\frac{p_2^2-p_1^2}{2M\hbar}\rho_{-+}(p_1,p_2)+ \\
&+ i\Omega_-\rho_{-e}(p_1,p_2-\hbar k)-i\Omega_+^*\rho_{e+}(p_1+\hbar k,p_2)+ \\
&+ i\Omega'_-\rho_{-e'}(p_1,p_2-\hbar k')-i\Omega'^*_+\rho_{e'+}(p_1+\hbar k',p_2), \\
\left[\frac{d}{dt}\rho_{ee'}(p_1,p_2)\right]_{Ham} &= i\left(\delta_L-\delta'_L+\frac{p_2^2-p_1^2}{2M\hbar}\right)\rho_{ee'}(p_1,p_2)- \\
&- i\Omega_+\rho_{-e'}(p_1-\hbar k,p_2)-i\Omega_-\rho_{+e'}(p_1+\hbar k,p_2)+ \\
&+ i\Omega'^*_+\rho_{e-}(p_1,p_2-\hbar k')+i\Omega'^*_-\rho_{e+}(p_1,p_2+\hbar k').
\end{aligned}
\tag{A.3}
$$

The terms describing the spontaneous emission from the upper level e to the lower levels g_- and g_+ are

$$
\left[\frac{d}{dt}\rho_{ee}(p_1,p_2)\right]_{\Gamma}=-\Gamma\rho_{ee}(p_1,p_2),
$$

$$\left[\frac{d}{dt}\rho_{e\pm}(p_1,p_2)\right]_\Gamma = -\frac{\Gamma}{2}\rho_{e\pm}(p_1,p_2),$$
$$\left[\frac{d}{dt}\rho_{ee'}(p_1,p_2)\right]_\Gamma = -\frac{\Gamma}{2}\rho_{ee'}(p_1,p_2), \tag{A.4}$$

$$\left[\frac{d}{dt}\rho_{--}(p_1,p_2)\right]_\Gamma = \left[\frac{d}{dt}\rho_{++}(p_1,p_2)\right]_\Gamma = \frac{\Gamma}{2}\int\limits_{-\hbar k}^{\hbar k} duH(u)\rho_{ee}(p_1+u,p_2+u).$$

Analogously, the terms describing the spontaneous emission from the upper level e' to the lower levels g_- and g_+ are

$$\left[\frac{d}{dt}\rho_{e'e'}(p_1,p_2)\right]_{\Gamma'} = -\Gamma'\rho_{e'e'}(p_1,p_2),$$
$$\left[\frac{d}{dt}\rho_{e'\pm}(p_1,p_2)\right]_{\Gamma'} = -\frac{\Gamma'}{2}\rho_{e'\pm}(p_1,p_2),$$
$$\left[\frac{d}{dt}\rho_{ee'}(p_1,p_2)\right]_{\Gamma'} = -\frac{\Gamma'}{2}\rho_{ee'}(p_1,p_2), \tag{A.5}$$
$$\left[\frac{d}{dt}\rho_{--}(p_1,p_2)\right]_{\Gamma'} = \left[\frac{d}{dt}\rho_{++}(p_1,p_2)\right]_{\Gamma'} = \frac{\Gamma'}{2}\int\limits_{-\hbar k'}^{\hbar k'} duH'(u)\rho_{e'e'}(p_1+u,p_2+u).$$

The terms corresponding to the decay from the upper level e' into the outside of the working configuration are

$$\left[\frac{d}{dt}\rho_{e'e'}(p_1,p_2)\right]_{\Gamma'_d} = -\Gamma'_d\rho_{e'e'}(p_1,p_2),$$
$$\left[\frac{d}{dt}\rho_{e'\pm}(p_1,p_2)\right]_{\Gamma'_d} = -\frac{\Gamma'_d}{2}\rho_{e'\pm}(p_1,p_2), \tag{A.6}$$
$$\left[\frac{d}{dt}\rho_{ee'}(p_1,p_2)\right]_{\Gamma'_d} = -\frac{\Gamma'_d}{2}\rho_{ee'}(p_1,p_2).$$

The generalized optical Bloch equations are obtained by adding the terms of Eqs. (A.3)–(A.6).

References

1. G. Alzetta, A. Gozzini, L. Moi, and G. Orriols, Nuovo Cimento B **36**, 5 (1976).
2. B. J. Dalton and P. L. Knight, in *Laser Physics, Lecture Notes in Physics*, ed. by J. D. Harvey and D. F. Walls, Springer, Berlin (1983), Vol. 182, p. 213.
3. H. I. Yoo and J. H. Eberly, Phys. Rep. **118**, 239 (1985).
4. E. Arimondo, in *Interaction of Radiation with Matter, Volume in Honor of Adriano Gozzini*, ed. by G. Alzetta, F. Bassani, and L. Radicati, Scuola Normale Superiore, Pisa, (1987), p. 343.

5. B. D. Agap'ev, M. B. Gornyi, and B. G. Matisov, Physics-Uspekhi **36**, 763 (1993).
6. E. Arimondo, in *Progress in Optics*, ed. by E. Wolf, Elsevier, Amsterdam (1996), XXXV, p. 257.
7. A. Aspect, E. Arimondo, R. Kaiser, N. Vansteenkiste, and C. Cohen-Tannoudji, Phys. Rev. Lett. **61**, 826 (1988).
8. F. Bardou, B. Saubamea, J. Lawall, K. Shimizu, O. Émile, C. Westbrook, A. Aspect, and C. Cohen-Tannoudji, C. R. Acad. Sci. Paris, Série II **318**, 877 (1994).
9. J. Lawall, F. Bardou, B. Saubamea, K. Shimizu, M. Leduc, A. Aspect, and C. Cohen-Tannoudji, Phys. Rev. Lett. **73**, 1915 (1994).
10. M. R. Doery, M. T. Widmer, M. J. Bellanca, W. F. Buell, T. H. Bergeman, H. Metcalf, and E. J. D. Vredenbregt, Phys. Rev. A **52**, 2295 (1995).
11. A. Aspect, E. Arimondo, R. Kaiser, N. Vansteenkiste, and C. Cohen-Tannoudji, J. Opt. Soc. Am. B **6**, 2112 (1989).
12. Y. Castin, H. Wallis, and J. Dalibard, J. Opt. Soc. Am. B **6**, 2046 (1989).
13. V. Z. Alekseev and D. D. Krylova, JETP Lett. **55**, 321 (1992).
14. V. Z. Alekseev and D. D. Krylova, Laser Phys. **2**, 781 (1992).
15. V. Z. Alekseev and D. D. Krylova, Opt. Commun. **95**, 319 (1993).
16. E. A. Korsunsky, D. V. Kosachiov, B. G. Matisov, Yu. V. Rozhdestvensky, L. Windholz, and C. Neureiter, Phys. Rev. A **48**, 1419 (1993).
17. F. Bardou, J. P. Bouchaud, O. Émile, A. Aspect, and C. Cohen-Tannoudji, Phys. Rev. Lett. **72**, 203 (1994).
18. M. R. Doery, R. Gupta, T. Bergeman, H. Metcalf, and E. J. D. Vredenbregt, Phys. Rev. A **51**, 2334 (1995).
19. S. Schaufler and V. P. Yakovlev, Laser Physics **6**, 414 (1996).
20. P. Marte, R. Dum, R. Taïeb, P. Zoller, M. S. Shahriar, and M. Prentiss, Phys. Rev. A **49**, 4826 (1994).
21. F. Shimizu, K. Shimizu, and H. Takuma, Jap. J. Appl. Phys. **26**, L1847 (1987).